Hydrogen Clathrate Structures in Rare Earth Hydrides at High Pressures: Possible Enroute to Room-temperature Superconductivity

Feng Peng,[1,2,3] Ying Sun,[3] Chris J. Pickard,[4] Richard J. Needs,[5] Qiang Wu,[6] and Yanming Ma[3,7,*]

[1]*Beijing Computational Science Research Center, Beijing 10084, China*
[2]*College of Physics and Electronic Information, Luoyang Normal University & Henan Key Laboratory of Electromagnetic Transformation and Detection, Luoyang 471022, China*
[3]*State Key Laboratory of Superhard Materials, College of Physics, Jilin University, Changchun 130012, China*
[4]*Department of Materials Science & Metallurgy, University of Cambridge, 27 Charles Babbage Road, Cambridge CB3 0FS, United Kingdom, and Advanced Institute for Materials Research, Tohoku University 2-1-1 Katahira, Aoba, Sendai 980-8577, Japan*
[5]*Theory of Condensed Matter Group, Cavendish Laboratory, J J Thomson Avenue, Cambridge CB3 0HE, United Kingdom*
[6]*National Key Laboratory of Shock Wave and Detonation Physics, Institute of Fluid Physics, CAEP, Mianyang 621900, China*
[7]*International Center of Future Science, Jilin University, Changchun 130012, China*

(Dated: July 22, 2017)

Room-temperature superconductivity has been a long-held dream and an area of intensive research. Recent experimental findings of superconductivity at 200 K in highly compressed hydrogen (H) sulfides have demonstrated the potential for achieving room-temperature superconductivity in compressed H-rich materials. We report first-principles structure searches for stable H-rich clathrate structures in rare earth hydrides at high pressures. The peculiarity of these structures lies in the emergence of unusual H cages with stoichiometries H_{24}, H_{29}, and H_{32}, in which H atoms are weakly covalently-bonded to one another, with rare earth atoms occupying the centers of the cages. We have found that high-temperature superconductivity is closely associated with H clathrate structures with large H-derived electronic densities of states at the Fermi level and strong electron-phonon coupling related to the stretching and rocking motions of H atoms within the cages. Strikingly, a Yttrium (Y) H_{32} clathrate structure of stoichiometry YH_{10} is predicted to be a potential room-temperature superconductor with an estimated T_c of up to 303 K at 400 GPa, as derived by direct solution of the Eliashberg equation.

PACS numbers: 74.70.Ad, 74.10.+v, 74.25.Jb, 74.62.Fj

At high pressures the lightest element, H, is suggested to form metallic solids with the high Debye temperature and strong electron-phonon coupling necessary for high-T_c phonon-mediated superconductivity [1, 2]. The superconductivity is supported by a number of calculations that have predicted a high T_c in the range 100-760 K in either molecular [3, 4] or atomic phases [5]. Unfortunately, low-temperature studies up to 388 GPa have not yet realized metallization of solid hydrogen [6]. Metallization of solid H at 495 GPa [7] has recently been reported, but additional experimental measurements are required to verify this claim. As an alternative, H-rich materials have been considered [8] since they can metallize at much lower pressures than are accessible to experiments. Extensive theoretical studies (e.g. Refs.[9–21]) have explored potential superconductivity in compressed H-rich materials. Encouragingly, the results suggest the possibility of high-T_c superconductivity in hydrides with estimated T_c values in the range 50-264 K [9–21]. The subsequent experimental observation of high-T_c superconductivity in the temperature ranges 30-150 K and 180-203 K for various temperature-annealed samples in highly compressed H_2S is remarkable [22]. These experiments were motivated by a theoretical prediction of high-T_c superconductivity in compressed solid H_2S [23] which excluded the possibility of dissociation of H_2S into S and H and opened up the possibility of synthesizing superconducting H_3S via compression of H_2S [24–26].

Two properties of metallic hydrides are particularly beneficial for promoting high-T_c superconductivity: (i) a large H-derived electronic density of states at the Fermi level, and (ii) large modifications of the electronic structure in response to the motion of the H atoms (electron-phonon coupling). It appears to be important to satisfy both of these criteria in hydrides with high H content in order to achieve high T_c values. However, the strategy of pursuing the highest possible H content may not always be the best solution. In reality, a number of hydrides with higher H content (e.g., AsH_8, MgH_{12}, and LiH_8, etc. Refs.[15, 27–29]) have been found not to exhibit higher T_c values than those containing relatively less H, such as CaH_6 and YH_6 [9, 10]. The key drawback of these H-rich structures lies in the appearance of H_2-like molecular units that attract many electrons from H atoms with low-lying energies away from the Fermi energy, which violates both criteria (i) and (ii). Another desirable property that is important for achieving high T_c superconductivity is that the structures should have

high symmetry. This appears to be a very general property that is not confined to metallic hydrides [30].

Synthesis of high-T_c superconducting hydrides requires the elimination of H_2-like molecular units from the structures. One possible route is to introduce electrons that are accepted by H_2 molecules which occupy the unfilled antibonding σ^* orbitals of the H_2 molecules, which would weaken the intramolecular H-H bonds and result in dissociation of H_2 [9, 30]. This is the physical origin of the stabilization of three-dimensional clathrate H_{24} cage structures, as first reported in CaH_6 [9] and later in YH_6 [10], where Ca and Y atoms occupy the center of the H_{24} cages and act as electron donors, while the H atoms are weakly covalently bonded to each other within the H_{24} cage. The H_{24} cage structure could be a useful compromise for achieving the largest possible number of H atoms, but without introducing molecular H_2 units into the structure. The high-T_c superconductivity arises from satisfying the above two criteria (i) and (ii) which has achieved theoretical T_c values of 235 K for CaH_6, and 264 K for YH_6, which is the highest theoretical T_c value achieved so far in a thermodynamically stable phase. Assuming MgH_6 adopts the same structure as CaH_6 does, an even higher T_c of 400 K was reported for MgH_6 [31], however, MgH_6 is known to be energetically unfavorable with respect to decomposition into MgH_4 and MgH_{12} [29].

In this work we seek binary metal hydrides that have even higher H content than CaH_6 and YH_6, while at the same time the structures should not contain H_2 molecules. For this purpose, the H lattices of hydrides should involve more electrons from the metal elements than they do in CaH_6 and YH_6. In this regard rare earth (RE) hydrides have come to our attention. On the one hand, RE elements such as Y in YH_6 can easily lose electrons due to their small electronegativities in the range of 1.0-1.36 on the Pauli scale [32], which is comparable to the value of 1.0 for Ca. On the other hand, RE elements can readily accommodate higher oxidation states (e.g., in 3+ or 4+ charge states) than that of Ca/Y (2+) in Ca/YH_6, which enables donation of more electrons to the H lattice.

Here we report an extensive exploration of the high-pressure phase diagrams of RE (Sc, Y, La, Ce, and Pr, etc.) hydrides, focusing on H-rich species by performing swarm-intelligence based CALYPSO [33, 34] structure searches. Some of the key clathrate structures were subsequently confirmed using the Ab Initio Random Structure Searching (AIRSS) approach [35, 36]. Our structure searches revealed that H clathrate structures could be formed in all of the RE hydrides studied. Besides the known H_{24} cage structure in REH_6, H-rich H_{29} and H_{32} cage structures were predicted in REH_9 and REH_{10} hydrides. Among them, the H_{32} cage structure in the temperature-stabilized YH_{10} clathrate is predicted to be a potential room-temperature superconductor with a T_c

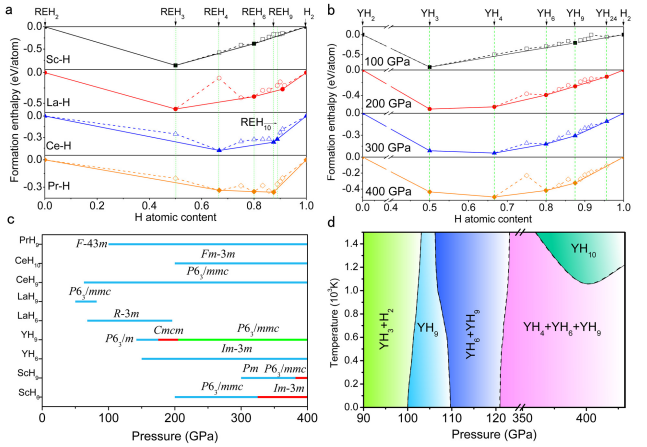

FIG. 1: (Color online) Phase stabilities of various H-rich RE hydrides (RE = Sc, Y, La, Ce, and Pr). (a) Enthalpies of formation of various H-rich RE hydrides at 200 GPa. (b) Enthalpies of formation of various H-rich Y hydrides under pressure. Dotted lines connect the data points, and solid lines denote the convex hull. (c) Predicted pressure-composition phase diagram of REH_6, REH_9, and REH_{10} clathrate structures. (d) Temperature versus pressure phase diagram of Y-H system. Dashed lines show the proposed phase boundaries.

of up to 303 K at 400 GPa, as derived by direct solution of the Eliashberg equation [37].

Our main structure searching results are depicted in the convex hull diagrams of Fig. 1 (a and b) and Supplementary Figs. S1-S5. The energetic stabilities of a variety of RE hydrides were evaluated from their formation enthalpies relative to the dissociation products of mixtures of REH_2 + H_2, where REH_2 is the known stable RE hydride at ambient pressure [38]. Fig. 1 (a and b) and Supplementary Figs. S1-S5 [39] show that the thermodynamically most stable stoichiometry varies with increasing atomic number of the RE metals. In the low-pressure regime (< 50 GPa), REH_3 (Figs. S1-S3) is the most stable species in the Sc-H, Y-H and La-H systems, while REH_4 (Figs. S4-S5) is the most stable in the Ce-H and Pr-H systems. The change in stoichiometry with pressure might result from the distinct oxidation states (e.g., 3+ for Sc, Y, and La, and 3+/4+ for Ce and Pr at ambient pressure). Besides the known REH_3 and REH_4 hydrides, the predicted REH_6 structures in the Sc-H and La-H systems adopt the same $Im\bar{3}m$ clathrate structure as in CaH_6 [9] and YH_6 [10] that consists of H_{24} cages as depicted in Fig. 2a. Substantially H-richer REH_9 and REH_{10} species exhibiting peculiar three-dimensional H clathrate structures of H_{29} and H_{32} cages were identified in most of the RE-H systems studied, as shown in Figs. 2b and 2c. The predicted stable pressure ranges at zero temperature for various clathrate structures are listed in Fig. 1c. We note that once temperature effects are included via quasi-harmonic free-energy calculations [55], the REH_{10} structure is also stabilized in Y-H systems at

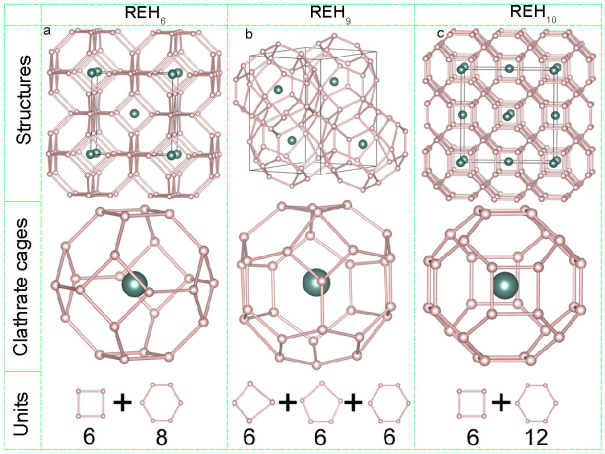

FIG. 2: (Color online) Clathrate structures of REH_6 (a), REH_9 (b), and REH_{10} (c). The small and large spheres represent H and RE atoms, respectively. The middle panel depicts the RE centered H_{24}, H_{29}, and H_{32} cages of REH_6, REH_9, and REH_{10}, respectively. Each H_{24}/H_{32} cage with O_h/D_{4h} symmetry contains six squares + eight hexagons/six squares + twelve hexagons. One H_{29} cage consists of six irregular squares + six pentagons + six hexagons.

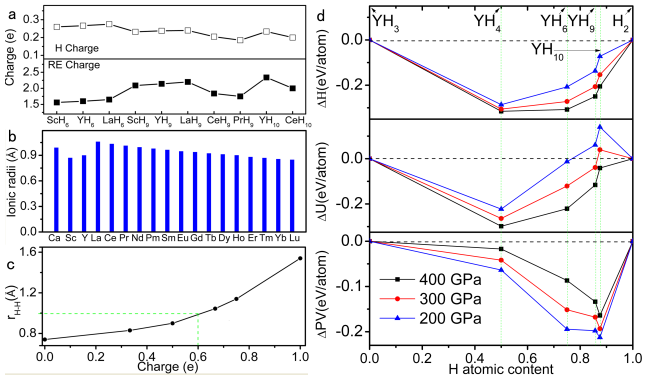

FIG. 3: (Color online) Formation mechanism of clathrate structures. (a) The anionic H and cationic RE charges are listed in the RE-H systems at 400 GPa. (b) Ionic radii for the RE elements are compared to those in Ca. (c) Variation of the H-H separation (r_{H-H}) in a H_2 molecule with the electrons accepted per H_2 molecule (see computational details in the Supplementary Material). (d) Formation enthalpies (top panel), internal energies (middle panel), and PV energy terms (bottom panel) for Y hydrides relative to YH_3 + H_2.

temperatures > 1,000 K, as shown in Fig. 1d. Interestingly, single H_{24} or H_{32} cages share a structural similarity with the C/Si_{24} [56, 57] or C_{32} [58] clusters that have been proposed theoretically for IVA group elements. In those cases C-C/Si-Si forms sp^3 hybridized bonds, in contrast to H-H bonding which lacks p orbitals. In addition, our structure searches predict other stable stoichiometries of REH_8 in Ce-H and Pr-H systems which have layered structures (Fig. S7) and LaH_{11} with a three-dimensional H net structure (Fig. S8). These structures are highly interesting and do not contain H_2 molecules either, but we do not discuss their physical properties since they only show superconductivity that is much weaker than in the H clathrate structures that are the main focus of our work.

We examine the chemical bonding of the REH_6, REH_9 and REH_{10} clathrate structures by calculating the electron localization functions (ELF) [59] (Fig. S9). The RE-H bonding is purely ionic in view of the absence of charge localization between RE and H, while a weakly covalent H-H interaction is evident via the observation of charge localization between the nearest-neighbor H atoms. Note that within the H_{24}, H_{29}, and H_{32} cages, the nearest H-H distances are very similar and are equal to 1.24 Å, 1.17 Å, and 1.08 Åat 200 GPa, respectively, which are much longer than in the H_2 gas molecule (0.74 Å) and slightly longer than the H-H distance (0.98 Å) [60] in monatomic H at 500 GPa. Subsequent Crystalline Orbital Hamiltonian Population calculations [61] were performed to confirm the H-H covalent bonding in these clathrate structures. The results (Figs. S10a and S10b) clearly reveal the occupancy of the H-H bonding states, which lends strong support to the existence of H-H covalent bonding in the structure. There is significant charge transfer from RE to H as derived from a Mulliken population analysis [62] (Fig. 3a). The charges on the H atoms do not change much with increasing H content, but the RE charges increase significantly and provide additional electrons to the H atoms which stabilizes the clathrate structure. The strong anion-cation interaction increases the Madelung energy of the ionic component of the RE-H bonding, which increases the stability of these clathrate structures.

The clathrate structures are likely to be stable only if they contain a certain optimal numbers of H atoms and electrons accepted per H_2 donated by the RE metals. Two H atoms readily form a chemical bond which reduces the energy, but once a H_2 molecule is formed, the H-H σ bonding orbital is fully occupied and the H_2 electrons accepted per H_2 will reside in the antibonding σ^* orbitals, which weakens the H-H σ bond [9, 30, 63]. Indeed, the H-H σ bond-length increases with the number of electrons from the RE elements in an H_2 molecule (Fig. 3c). If the number of electrons accepted per H_2 molecule reaches about 0.6e, the H_2 molecule dissociates as the H-H bond length increases to about 1.0 Å, which is similar to the H-H distance (0.98 Å) in monatomic H at 500 GPa [60]. This model calculation suggests that once an optimal compromise between the number of H_2 molecules and electrons they accept is achieved, an alternative lower energy structure (e.g., clathrate structure) appears. Here, the nearest H-H distances for the REH_6 and REH_9/H_{10} clathrate structures are ∼1.2 and 1.0 Å, corresponding to a number accepted electrons of 0.7e and 0.6e per H_2, respectively. Our structure searches have identified an

extremely H-rich species of YH_{24} (Fig. S11), however, the H atoms remains in a molecular form in which the electronic charge accepted of 0.13e per H_2 is too small to destabilize the H_2 molecule.

To probe the thermodynamical origins of the stabilization of these clathrate structures, we chose the Y-H system as an example and present data in Fig. 3d for the enthalpies ΔH, the internal energies ΔU, and the pressure-volume term ΔPV. We see that ΔU increases with increasing H content under pressure, while the ΔPV term is reduced and the H-rich clathrate structures YH_6 and YH_9 tend to be stable and lie on the convex hull (see ΔH in Fig. 3d). The substantial reduction in volume under pressure leads to the stability of H-rich clathrate structures. We further examined all the clathrate structures, and surprisingly found that the RE-H distances in REH_6, REH_9, and REH_{10} are nearly equal, with a value of ~1.9 Å, which is close to the sum of the atomic radius (0.79 Å) of H and the ionic radii of RE atoms (in the range 0.84-1.08 Å, Fig. 3b). This observation indicates that the atoms in these clathrate structures are densely packed, which gives a natural explanation of the much reduced ΔPV term (bottom panel in Fig. 3d) once the clathrate structure is stabilized. Indeed, by careful inspection of 500 low-enthalpy structures generated by our searches for YH_9 at 300 GPa (Fig. S12), we found that the clathrate H_{29} structure has the smallest volume (23.16 $Å^3$ per formula unit) among those studied.

The H clathrate structures of REH_6, REH_9, and REH_{10} are metallic as seen from the calculated electronic band structures and densities of states (Fig. S13 and S14). The electronic density of states at the Fermi level is typically large and is dominated by the contribution from H atoms. To examine potential superconductivity in the clathrate structures, lattice phonons and electron-phonon coupling (EPC) calculations were carried out using linear response theory [64]. Encouragingly, the resulting EPC parameters λs of YH_9 and YH_{10} are quite large and reach values of 4.42 and 2.41 at 150 and 400 GPa, respectively. Besides the H-derived high density of states at the Fermi level that is associated with a Van Hove singularity at the Γ point (Fig. S14), the large λ values are mainly associated with in-plane stretching, in-plane rocking, and out-of-plane rocking vibrations of H clathrate cages (Fig. S15). The Eliashberg equation [37] gives a better description of systems with strong electron-phonon coupling for $\lambda > 1.5$. We have therefore used the Eliashberg equation to predict superconductivity in the clathrate structures using the calculated logarithmic average frequency (ω_{log}) and typical Coulomb pseudopotential parameters (μ^*) from 0.1 to 0.13. The resulting T_c values are 276 K (253 K for $\mu^* = 0.13$) and 303 K (287 K for $\mu^* = 0.13$) using $\mu^* = 0.1$ for YH_9 at 150 GPa and YH_{10} at 400 GPa, respectively. We also investigated potential superconductivity in other clathrate structures (Fig. 4) and predicted T_c values for ScH_6 and ScH_9 as high as ~150 K, although for LaH_9, CeH_9, CeH_{10} and PrH_9 they are much lower at < 56 K (Fig. 4) due to the introduction of much heavier elements which reduce BCS superconductivity.

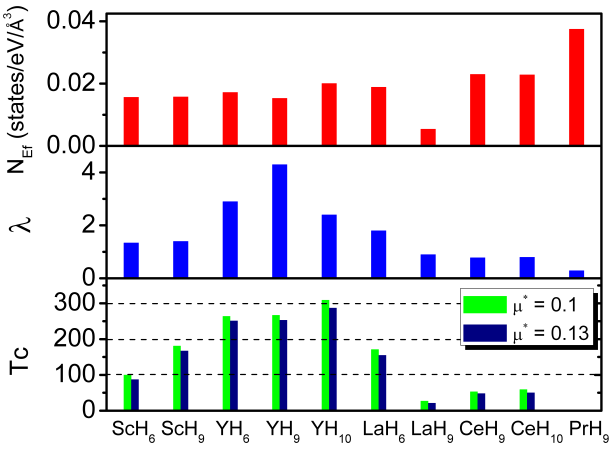

FIG. 4: (Color online) Calculated electronic DOS of H at the Fermi level (N_{Ef}) per $Å^3$ (top panel), the EPC parameter λ (middle panel), and T_c (bottom panel) of various clathrate structures at high pressures. The pressure values chosen within their stable pressure ranges of the phases are 300, 400, 120, 150, 400, 100, 50, 100, 200, and 100 GPa for ScH_6, ScH_9, YH_6, YH_9, YH_{10}, LaH_6, LaH_9, CeH_9, CeH_{10} and PrH_9, respectively.

Our extensive structure searches for RE (RE = Sc, Y, La, Ce, and Pr) hydrides have revealed the appearance of stable clathrate structures in REH_6, REH_9, and REH_{10}. These structures have extended our searches into other RE (RE = Nd, Pm, Sm, Eu, Gd, Tb, Dy, Ho, Er, Tm, Yb, and Lu) hydrides using density-functional-theory calculations and substituting the RE elements into the known REH_6, REH_9, and REH_{10} structures (Supplementary Figs. S16-S27). Our results show that clathrate structures often emerge in these RE hydrides. Stabilization of clathrate structures using RE hydrides at high pressures might therefore be a widespread phenomenon.

Two families of binary hydrides (i.e., nonmetals with high electronegativity and metals hydrides) are promising candidates for high-T_c superconductivity. For nonmetal hydrides in which H is able to form covalent bonds with nonmetallic elements, the three-dimensional covalently-bonded H structure appears only in the high-T_c H_3S [14] and H_3Se [65] materials. For metal hydrides in which bonding between H and metallic elements is purely ionic, we emphasize that H-H bonding in three-dimensional clathrate structures established for RE hydrides are potential high-T_c superconductors that present our greatest hope for achieving room-T_c superconductivity. Future theoretical searches for high-T_c superconductors are expected to investigate ternary or quaternary hydrides which have not been well-explored to date, although such structure searches can be challeng-

ing since their cost increases rapidly with the number of atoms and atomic species.

In conclusion, we have used extensive first-principles structure searches to establish the pressure-induced formation of H clathrate structures that contain H_{24}, H_{29}, and H_{32} cages with RE atoms at the centre of the H-rich RE hydrides studied. The origin of the stabilization of these clathrate structures is related to their densely-packed structures via a much reduced PV energy term which achieves a near-optimal compromise between the number of H atoms and the electrons donated by RE atoms in the structure. The clathrate structures exhibit potential high-T_c superconductivity that originates from the large H-derived electron density of states at the Fermi level and the strong electron-phonon coupling which is related to the motion of H atoms within the cages, among which YH_{10} is predicted to be a potential room temperature superconductor with a T_c of up to 303 K at 400 GPa. Our work will stimulate future high-pressure experimental work on synthesis of these clathrate structures to explore the high-T_c superconductivity and the peculiar chemical bondings involved. Direct chemical reactions of RE metals and H in laser-heated diamond-anvil-cell experiments might be able to overcome the kinetic barriers and achieve synthesis of these interesting hydrides.

We acknowledge funding support from Science Challenge Project at No. TZ2016001, the National Natural Science Foundation of China under Grant No. 11534003, and the National Key Research and Development Program of China under Grant No. 2016YFB0201200. We also thank China Postdoctoral Science Foundation under 2016M590033, the Natural Science Foundation of Henan Province Grant No. 162300410199, Program for Science and Technology Innovation Talents in University of Henan Province Grant No. 17HASTIT015 and Open Project of the State Key Laboratory of Superhard Materials, Jilin University under No. 201602. R.J.N. acknowledges funding from the Engineering and Physical Sciences Research Council (EPSRC) of the UK under grant [EP/J017639/1]. C.J.P. is supported by a Royal Society Wolfson Research Merit Award. Computational resources were provided by the high performance computing center of Jilin University, Tianhe2-JK in the Beijing Computational Science Research Center, and the High Performance Computing Service at the University of Cambridge and the Archer facility of the UK's national high-performance computing service, for which access was obtained via the UKCP consortium [EP/P022596/1].

* Electronic address: mym@jlu.edu.cn

[1] E. Wigner and H. B. Huntington, J. Chem. Phys. **3**, 764 (1935).
[2] N. W. Ashcroft, Phys. Rev. Lett. **21**, 1748 (1968).
[3] P. Cudazzo, G. Profeta, A. Sanna, A. Floris, A. Continenza, S. Massidda, and E. Gross, Phys. Rev. Lett. **100**, 257001 (2008).
[4] L. Zhang, Y. Niu, Q. Li, T. Cui, Y. Wang, Y. Ma, Z. He, and G. Zou, Solid State Commun. **141**, 610 (2007).
[5] J. M. McMahon and D. M. Ceperley, Phys. Rev. B **84**, 144515 (2011).
[6] P. Dalladay-Simpson, R. T. Howie, and E. Gregoryanz, Nature **529**, 63 (2016).
[7] R. P. Dias and I. F. Silvera, Science **355**, 715 (2017).
[8] N. W. Ashcroft, Phys. Rev. Lett. **92**, 187002 (2004).
[9] H. Wang, S. T. John, K. Tanaka, T. Iitaka, and Y. Ma, Proc. Natl. Acad. Sci. USA **109**, 6463 (2012).
[10] Y. Li, J. Hao, H. Liu, S. T. John, Y. Wang, and Y. Ma, Sci. Rep. **5**, 9948 (2015).
[11] M. Martinez-Canales, A. R. Oganov, Y. Ma, Y. Yan, A. O. Lyakhov, and A. Bergara, Phys. Rev. Lett. **102**, 087005 (2009).
[12] Y. Li, G. Gao, Y. Xie, Y. Ma, T. Cui, and G. Zou, Proc. Natl. Acad. Sci. USA **107**, 15708 (2010).
[13] G. Gao, A. R. Oganov, A. Bergara, M. Martinez-Canales, T. Cui, T. Iitaka, Y. Ma, and G. Zou, Phys. Rev. Lett. **101**, 107002 (2008).
[14] D. Duan, Y. Liu, F. Tian, D. Li, X. Huang, Z. Zhao, H. Yu, B. Liu, W. Tian, and T. Cui, Sci. Rep. **4**, 6968 (2014).
[15] Y. Xie, Q. Li, A. R. Oganov, and H. Wang, Acta Crystallog C **70**, 104 (2014).
[16] D. Zhou, X. Jin, X. Meng, G. Bao, Y. Ma, B. Liu, and T. Cui, Phys. Rev. B **86**, 014118 (2012).
[17] Z. Wang, Y. Yao, L. Zhu, H. Liu, T. Iitaka, H. Wang, and Y. Ma, J. Chem. Phys. **140**, 124707 (2014).
[18] X. Feng, J. Zhang, G. Gao, H. Liu, and H. Wang, RSC Adv. **5**, 59292 (2015).
[19] J. S. Tse, Y. Yao, and K. Tanaka, Phys. Rev. Lett. **98**, 117004 (2007).
[20] G. Gao, A. R. Oganov, P. Li, Z. Li, H. Wang, T. Cui, Y. Ma, A. Bergara, A. O. Lyakhov, and T. Iitaka, Proc. Natl. Acad. Sci. USA **107**, 1317 (2010).
[21] V. V. Struzhkin, Physica C **514**, 77 (2015).
[22] A. P. Drozdov, M. I. Eremets, I. A. Troyan, V. Ksenofontov, and S. I. Shylin, Nature **525**, 73 (2015).
[23] Y. Li, J. Hao, H. Liu, Y. Li, and Y. Ma, J. Chem. Phys. **140**, 174712 (2014).
[24] D. Duan, X. Huang, F. Tian, D. Li, H. Yu, Y. Liu, Y. Ma, B. Liu, and T. Cui, Phys. Rev. B **91**, 180502 (2015).
[25] Y. Li, L. Wang, H. Liu, Y. Zhang, J. Hao, C. J. Pickard, J. R. Nelson, R. J. Needs, W. Li, and Y. Huang, Phys. Rev. B **93**, 020103 (2016).
[26] I. Errea, M. Calandra, C. J. Pickard, J. Nelson, R. J. Needs, Y. Li, H. Liu, Y. Zhang, Y. Ma, and F. Mauri, Phys. Rev. Lett. **114**, 157004 (2015).
[27] Y. Fu, X. Du, L. Zhang, F. Peng, M. Zhang, C. J. Pickard, R. J. Needs, D. J. Singh, W. Zheng, and Y. Ma, Chem. Mater. **28**, 1746 (2016).
[28] E. Zurek, R. Hoffmann, N. W. Ashcroft, A. R. Oganov, and A. O. Lyakhov, Proc. Natl. Acad. Sci. USA **106**, 17640 (2009).
[29] D. C. Lonie, J. Hooper, B. Altintas, and E. Zurek, Phys. Rev. B **87**, 054107 (2013).
[30] L. Zhang, Y. Wang, J. Lv, and Y. Ma, Nat. Rev. Mater. **2**, 17005 (2017).
[31] A. P. Durajski and R. Szczeniak, Supercond. Sci. Technol. **27**, 115012 (2014).
[32] A. L. Allred, J. Inorg. Nuclear Chem. **17**, 215 (1961).

[33] Y. Wang, J. Lv, L. Zhu, and Y. Ma, Phys. Rev. B **82**, 094116 (2010).

[34] Y. Wang, J. Lv, L. Zhu, and Y. Ma, Comput. Phys. Commun. **183**, 2063 (2012).

[35] C. J. Pickard and R. J. Needs, Phys. Rev. Lett. **97**, 045504 (2006).

[36] C. J. Pickard and R. J. Needs, J. Phys.: Condens. Matter **23**, 053201 (2011).

[37] G. M. Eliashberg, Sov. Phys. JETP **11**, 696 (1960).

[38] Y. Wang and M. Y. Chou, Phys. Rev. B **51**, 7500 (1995).

[39] See Supplemental Material at http://*** for computational details, electronic structures, phonon dispersion curves, phase diagrams, and structural parameters of all predicted RE-H compounds, which includes Refs.[40–54].

[40] J. Lv, Y. Wang, L. Zhu, and Y. Ma, Phys. Rev. Lett. **106**, 015503 (2011).

[41] L. Zhu, H. Wang, Y. Wang, J. Lv, Y. Ma, Q. Cui, Y. Ma, and G. Zou, Phys. Rev. Lett. **106**, 145501 (2011).

[42] Y. Wang, H. Liu, J. Lv, L. Zhu, H. Wang, and Y. Ma, Nat. Commun. **2**, 563 (2011).

[43] H. Wang, S. T. John, K. Tanaka, T. Iitaka, and Y. Ma, Proc. Natl. Acad. Sci. USA **109**, 6463 (2012).

[44] X. Wang, Y. Wang, M. Miao, X. Zhong, J. Lv, T. Cui, J. Li, L. Chen, C. J. Pickard, and Y. Ma, Phys. Rev. Lett. **109**, 175502 (2012).

[45] L. Zhu, H. Liu, C. J. Pickard, G. Zou, and Y. Ma, Nat. Chem. **6**, 644 (2014).

[46] C. L. Guillaume, E. Gregoryanz, O. Degtyareva, M. I. McMahon, M. Hanfland, S. Evans, M. Guthrie, S. V. Sinogeikin, and H.-K. Mao, Nat. Phys. **7**, 211 (2011).

[47] G. Kresse, Phys. Rev. B **54**, (1996).

[48] M. D. Segall, P. J. Lindan, M. A. Probert, C. J. Pickard, P. J. Hasnip, S. J. Clark, and M. C. Payne, J. Phys.: Condens. Matter **14**, 2717 (2002).

[49] D. Sanchez-Portal, E. Artacho, and J. M. Soler, Solid State Commun. **95**, 685 (1995).

[50] R. S. Mulliken, J. Chem. Phys. **23**, 1833 (1955).

[51] M. Frisch, G. W. Trucks, H. Schlegel, G. E. Scuseria, M. A. Robb, J. R. Cheeseman, J. A. Montgomery, T. Vreven, K. N. Kudin, and J. Burant, Gaussian 03, Revision C. 02 (2008).

[52] B. Y. Ao, X. L. Wang, P. Shi, P. H. Chen, X. Q. Ye, X. C. Lai, J. J. Ai, and T. Gao, Int. J. Hydrogen Energy **37**, 5108 (2012).

[53] P. Blaha, K. Schwarz, P. Sorantin, and S. B. Trickey, Comput. Phys. Commun. **59**, 399 (1990).

[54] F. Birch, Phys. Rev. **71**, 809 (1947).

[55] A. Togo, F. Oba, and I. Tanaka, Phys. Rev. B **78**, 134106 (2008).

[56] R. O. Jones, J. Chem. Phys. **110**, 5189 (1999).

[57] N. Jaussaud, M. Pouchard, P. Gravereau, S. Pechev, G. Goglio, C. Cros, A. San Miguel, and P. Toulemonde, Inorg. Chem. **44**, 2210 (2005).

[58] Q. Sun, Q. Wang, J. Z. Yu, K. Ohno, and Y. Kawazoe, J. Phys.: Condens. Matter **13**, 1931 (2001).

[59] A. D. Becke and K. E. Edgecombe, J. Chem. Phys. **92**, 5397 (1990).

[60] J. M. McMahon and D. M. Ceperley, Phys. Rev. Lett. **106**, 165302 (2011).

[61] V. L. Deringer, A. L. Tchougreff, and R. Dronskowski, J. Phys. Chem. A **115**, 5461 (2011).

[62] M. D. Segall, R. Shah, C. J. Pickard, and M. C. Payne, Phys. Rev. B **54**, 16317 (1996).

[63] V. Labet, P. Gonzalez-Morelos, R. Hoffmann, and N. W. Ashcroft, J. Chem. Phys. **136**, 074501 (2012).

[64] S. Baroni, P. Giannozzi, and A. Testa, Phys. Rev. Lett. **58**, 1861 (1987).

[65] S. Zhang, Y. Wang, J. Zhang, H. Liu, X. Zhong, H.-F. Song, G. Yang, L. Zhang, and Y. Ma, Sci. Rep. **5**, 15433 (2015).